Water Research 204 (2021) 117625

Contents lists available at ScienceDirect

Water Research

journal homepage: www.elsevier.com/locate/watres

Metagenomic insights into co-proliferation of *Vibrio* spp. and dinoflagellates *Prorocentrum* during a spring algal bloom in the coastal East China Sea

Daehyun Daniel Kim [b,1], Lingling Wan [a,1], Xiuyun Cao [a], Daniela Klisarova [c,d], Dimitar Gerdzhikov [d], Yiyong Zhou [a], Chunlei Song [a,*], Sukhwan Yoon [b,*]

[a] Key Laboratory of Algal Biology, State key laboratory of Freshwater Ecology and Biotechnology, Institute of Hydrobiology, Chinese Academy of Sciences, Wuhan, 430072, China
[b] Department of Civil and Environmental Engineerimng, KAIST, Daejeon, 34141, Republic of Korea
[c] Department of Anatomy, Histology, Cytology and Biology, Faculty of Medicine, Medical University, Pleven, 5800, Bulgaria
[d] Institute of Fish Resources, 9000 Varna, Bulgaria

ARTICLE INFO

Keywords:
Harmful algal bloom
Microbiome
Metagenomics
Prorocentrum
Vibrio
DNRA

ABSTRACT

Coastal harmful algal blooms (HABs), commonly termed 'red tides', have severe undesirable consequences to the marine ecosystems and local fishery and tourism industries. Increase in nitrogen and/or phosphorus loading is often regarded as the major culprits of increasing frequency and intensity of the coastal HAB; however, fundamental understanding is lacking as to the causes and mechanism of bloom formation despite decades of intensive investigation. In this study, we interrogated the prokaryotic microbiomes of surface water samples collected at two neighboring segments of East China Sea that contrast greatly in terms of the intensity and frequency of *Prorocentrum*-dominated HAB. Mantel tests identified significant correlations between the structural and functional composition of the microbiomes and the physicochemical state and the algal biomass density of the surface seawater, implying the possibility that prokaryotic microbiota may play key roles in the coastal HAB. A conspicuous feature of the microbiomes at the sites characterized with high trophic state index and eukaryotic algal cell counts was disproportionate proliferation of *Vibrio* spp., and their complete domination of the functional genes attributable to the dissimilatory nitrate reduction to ammonia (DNRA) pathway substantially enriched at these sites. The genes attributed to phosphorus uptake function were significantly enriched at these sites, presumably due to the P_i-deficiency induced by algal growth; however, the profiles of the phosphorus mineralization genes lacked consistency, barring any conclusive evidence with regard to contribution of prokaryotic microbiota to phosphorus bioavailability. The results of the co-occurrence network analysis performed with the core prokaryotic microbiome supported that the observed proliferation of *Vibrio* and HAB may be causally associated. The findings of this study suggest a previously unidentified association between *Vibrio* proliferation and the *Prorocentrum*-dominated HAB in the subtropical East China Sea, and opens a discussion regarding a theoretically unlikely, but still possible, involvement of *Vibrio*-mediated DNRA in *Vibrio-Prorocentrum* symbiosis. Further experimental substantiation of this supposed symbiotic mechanism may prove crucial in understanding the dynamics of explosive local algal growth in the region during spring algal blooms.

1. Introduction

Today, many coastal regions across the globe suffer from harmful algal blooms (HAB), more widely known as the layman's term 'red tides' (Anderson et al., 2012). The East China Sea off the southeast coast of China has been one of the regions most severely affected by HAB since the 1980s (Tang et al., 2006). Since the turn of millennium, the major culprits of HAB in the East China Sea have shifted to the dinoflagellates *Prorocentrum* spp., a group of fast-growing phototrophic algae widespread in coastal waters across the globe (Heil et al., 2005). The species

* Corresponding authors.
E-mail addresses: clsong@ihb.ac.cn (C. Song), syoon80@kaist.ac.kr (S. Yoon).
[1] Equal contribution and co-first author.

https://doi.org/10.1016/j.watres.2021.117625
Received 29 June 2021; Received in revised form 24 August 2021; Accepted 27 August 2021
Available online 3 September 2021

prevalent in HAB in East China Sea, which had been named *P. donghaiense*, is neither morphologically nor genotypically clearly distinguishable from other *Prorocentrum* species with worldwide distribution, e.g., *P. dentatum* and *P. obtusidens* (Lu et al., 2005; Shin et al., 2019). Although toxin production by this particular species has not been reported, the possibility cannot be totally ruled out, as several *Prorocentrum* species have been observed to produce okadaic acid, dinophysistoxin-1, and prorocentrolide (Ben-Gharbia et al., 2016; Nascimento et al., 2017). Even apart from toxin production, intense *Prorocentrum* blooms cause substantial detrimental impacts to the local marine and estuarine ecosystems by means of oxygen depletion, alteration of pH, and/or light attenuation, which are typical for high-biomass algal blooms (Anderson et al., 2012; Azanza et al., 2005; Gallegos and Bergstrom, 2005). Such ecological damage, as well as aesthetic deterioration due to coloration and putrefaction accompanied with the blooms, have caused immense damage to the local tourism, fishing, and aquaculture industries (Yu et al., 2018).

The annually repetitive nature of the *Prorocentrum* algal bloom in the East China Sea, as well as explosive growths of *P. donghaiense* observed during progressions of the algal blooms endemic to the region, suggests that *in situ* growth is more important than vertical and/or horizontal migration in understanding the mechanisms of bloom dynamics in the region (Li et al., 2011; Tang et al., 2006). As *P. donghaiense* is primarily a photoautotrophic organism with carbon needs mostly fulfilled from uptake of inorganic carbon, the environmental factors regarded to be crucial to its overgrowth during the bloom events are presumably availability of nitrogen and phosphorus, as suggested by previous laboratory observations (Anderson et al., 2012; Glibert et al., 2008; Varkitzi et al., 2010). Although several published data collected from the East China Sea suggest potential correlations between nitrogen and phosphorus availability and *P. donghaiense* blooms, conclusive experimental evidences are still lacking, and it is yet unclear whether or which specific forms of nitrogen and phosphorus support rapid growth of *P. donghaiense* (Li et al., 2010; Zhou et al., 2017). As such, the decades-long question as to whether or how relief of nitrogen and/or phosphorus limitation initiates *P. donghaiense* bloom remains unanswered.

In this study, we approached this same old question from a different perspective, exploring the possibility that the sea surface microbiome may play a key role in formation and progression of *Prorocentrum* blooms. Diverse bacterial and archaeal constituents of the sea surface microbiota are involved with cycling of nitrogen and phosphorus (Kuypers et al., 2018). In the euphotic zone, generally characterized by supple sunlight and oxygen availability, photosynthetic cyanobacteria fix atmospheric nitrogen to ammonium and organic nitrogen, and diverse bacteria and archaea catalyze aerobic mineralization of organic N and oxidation of NH_3 and NO_2^- (Dore and Karl, 1996; Michael Beman et al., 2012; Wankel et al., 2007). Typically, NO_3^- is often the most abundant form of nitrogen at the sea surface due to its oxidizing condition (Mahmud et al., 2020; Patey et al., 2008). The microbial reactions perceived as predominantly anaerobic, e.g., denitrification, anaerobic ammonia oxidation (anammox), and dissimilatory nitrate/nitrite reduction to ammonium (DNRA), may also occur during periodic hypoxia, e.g., nocturnal anoxic spells during high-biomass algal blooms and periods of massive biomass decay following demise of algal blooms (Conley et al., 2011; Turner et al., 2015). Such microbial mediated nitrogen transformation reactions may affect nitrogen supply to phytoplankton, as they may alter the overall nitrogen availability, as well as nitrogen speciation. As nitrogen is often regarded as the limiting nutrient for algal growth during rapid blooms and previous laboratory experiments have shown that certain nitrogen species are favored by *Prorocentrum* spp. over others, investigations into these microbially mediated nitrogen-transformations may help improve understanding of the bloom dynamics in the East China Sea (Fan et al., 2003; Heil et al., 2005; Varkitzi et al., 2010).

Less predictable is the influence of microbiota on HAB via alteration of the marine phosphorus cycle, given the patchy ecophysiological understanding of marine microbial phosphorus metabolism. Previous metagenomic analyses have revealed abundance and omnipresence of diverse *phoA*-, *phoD*-, and *phoX*-type alkaline phosphatases (AP) and C-P lyases and hydrolases in seawater microbiomes, which have been known to be involved with disintegration of inorganic phosphorus (P_i) from phosphoesters and phosphonates (Luo et al., 2009; Luo and Moran, 2013; Sebastian and Ammerman, 2009). Expressions of these organic phosphorus metabolizing enzymes are generally perceived to be under *Pho* regulon control, such that they are expressed only under P_i-deficiency; however, P_i-insensitive expression and activity of alkaline phosphatases and C-P hydrolases have been experimentally demonstrated in both *in situ* and laboratory experiments (Chin et al., 2018; Suzumura et al., 2012). Thus, bacterial mineralization of organic phosphorus may enrich the inorganic phosphorus pool *in situ* and increase phosphorus bioavailability to phytoplanktons, contributing to formation of HAB (Hoppe, 2003; Luo et al., 2009; Thomson et al., 2019). Marine eukaryotic phytoplankton, including *Prorocentrum* spp., also synthesize active AP (Hoppe, 2003; Labry et al., 2005; Ou et al., 2020); however, a recent field study conducted in the East China Sea during a late-spring *P. donghaiense* bloom showed that the bacterial fraction accounted for the majority of AP activity and that the contribution of eukaryotic algae was minimal (Mo et al., 2020).

Here, a comparative survey of the sea surface microbiomes was performed at two neighboring coastal seas off the coastline of Fujian Province in southeastern China. The sea surrounding Pingtan Island, hereafter referred to as Pingtan Sea, has been regularly and frequently affected by *P. donghaiense* blooms. In contrast, Xiamen Bay ~200 km to the southwest has stayed mostly free of *Prorocentrum* spp., although occasional occurrences of moderate diatom and dinoflagellate blooms have been reported (Zhuo, 2018). During a typical spring dinoflagellate bloom event in the Pingtan Sea in 2019, surface seawater samples were collected from five locations in Pingtan Sea and three locations in Xiamen Bay, and the physicochemical properties of the seawater and population densities and compositions of the eukaryotic algae were analyzed. The microbiomes of these seawater samples were then analyzed with shotgun metagenome sequencing. The compositional and functional features of the microbiomes were analyzed, with particular emphasis on those relating to nitrogen and phosphorus metabolism and statistically associated with the severity of HAB in the region. The findings from the comparative metagenomics analysis warrant further investigation into interactions between key microbial groups, e.g., *Vibrio* spp., and eukaryotic algae, for a more complete understanding of HAB dynamics in coastal seas.

2. Materials and methods

2.1. Sample collection and in situ treatment and characterization

Sampling was performed at five locations along the coast of Pingtan Island (25°28′-25°36′ N, 119°49′-119°52′ E) and three coastal locations in the Xiamen Bay (24°25′-24°36′ N, 118°0′-118°10′ E) in the mornings of April 27 and 29, 2018, respectively (Fig. 1a). Bulk seawater samples were collected from the surface layer (0-1 m depth) using hydrophores. The physicochemical properties of the seawater samples, including water temperature, dissolved oxygen concentration, conductivity, salinity, oxidation-reduction potential and pH, were measured on site immediately after sampling, using Professional Plus handheld multiparameter meter (YSI Inc., Yellow Springs, OH). Secchi disk transparency (SD) was determined on site according to the standard protocol (Tyler, 1968). Ten liters of each seawater sample was filtered through a phytoplankton net with 20 μm mesh size (Xuanmingyu, Wuhan, China) and one liter of the filtrate was passed through a 0.22-μm membrane filter to collect biomass (Merck Millipore, Burlington, MA). The phytoplankton nets and membrane filters were preserved in 2% formalin solution for transport to the Institute of Fish Resources in Varna, Bulgaria,

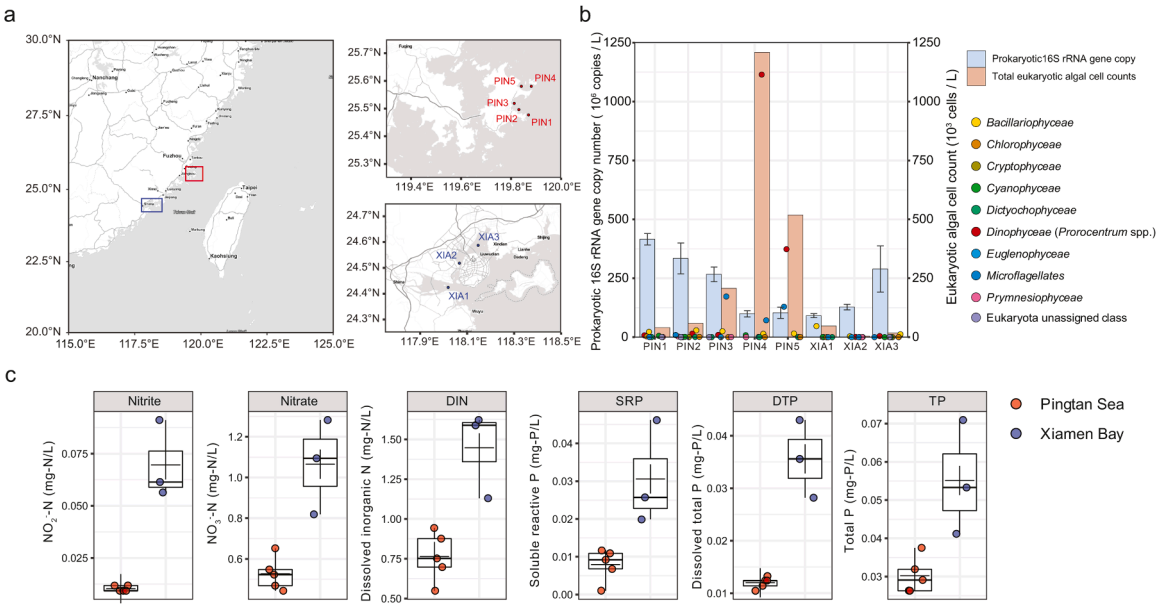

Fig. 1. Characterization of the sampling sites along the coastline of Pingtan Island (PIN1-5) and in Xiamen Bay (XIA1-3). (a) Geographical locations of the sampling sites in Pingtan Sea (PIN1-5) and Xiamen Bay (XIA1-3). (b) Populations of eukaryotic algae determined via direct microscopic counting of morphologically classified algal cells and 16S rRNA genes copy numbers as estimates of prokaryotic populations, determined with qPCR assays comprehensively targeting bacterial and archaeal 16S rRNA genes. (c) Nitrogen and phosphorus contents of the surface seawater collected from the sampling sites. Each dot represents a sampling site.

where the resuspended phytoplankton cells were examined with an Olympus BX43 phase contrast microscope (Tokyo, Japan) (Olenina et al., 2006). The phytoplankton cells resuspended from the phytoplankton nets were used for exhaustive identification of phytoplankton taxa, and algal cell counting was performed with the membrane filter retentates. Wet algal biomass was estimated from biovolume of phytoplankton cells calculated using geometric formulas (Edler, 1979; Olenina et al., 2006). The remaining phytoplankton net filtrate was transported to the laboratory at Wuhan Institute of Hydrobiology in ice-filled coolers for DNA extraction.

Further characterization of the seawater samples was performed in the laboratory. Portions of bulk water samples were filtered through 0.22-μm membrane filters (Merck Millipore) for quantification of dissolved nitrogen and phosphorus species. The NH_4^+-N, NO_3^--N, and NO_2^--N concentrations were determined colorimetrically as previously described (Greenberg et al., 2012). The dissolved inorganic nitrogen (DIN) concentration was calculated as the sum of the concentrations of these three nitrogen species. The soluble reactive phosphorus (SRP) concentration was determined using the molybdate blue method (Murphy and Riley, 1962). These measurements were repeated with the filtrates digested for 0.5 h with 5% alkaline persulphate solution (pH 12) for determination of the dissolved total nitrogen and dissolved total phosphorus (DTP) concentrations inclusive of the organic fractions (Langner and Hendrix, 1982). Unfiltered seawater samples were processed identically for determination of the total nitrogen (TN) and total phosphorus (TP) contents. The chlorophyll *a* contents (Chl *a*) were determined using the ethanol extraction method (Nusch, 1980). The trophic state index (TSI) was calculated from Chl *a*, SD and TP as previously described (Carlson, 1977).

2.2. DNA extraction and processing

In the laboratory, 1-1.5 L of each phytoplankton net-filtered seawater was filtered with a sterile 0.22-μm membrane filter (Merck Millipore, Burlington, MA) and the filters were immediately stored at -80°C. DNA was extracted from the filter retentate with the CTAB method, and the purity and quantity of the extracted DNA was assessed with the Qubit® 2.0 Fluorometer (Thermo Fisher Scientific, Waltham, MA) (Griffith et al., 2009; Raimundo et al., 2018; Trojánek et al., 2018). Each DNA sample was disrupted using a Covaris S2 sonicator (Woburn, MA). Sequencing libraries were generated using the TruSeq Nano DNA HT sample preparation kit (Illumina, San Diego, CA). The shotgun metagenome libraries were sequenced with an Illumina NovaSeq-PE150 platform, generating 150-bp paired-end reads with a targeted throughput of 12 Gb per sample. The raw sequence data have been deposited in NCBI SRA database under the accession number PRJNA739281.

Quantitative PCR (qPCR) assay targeting the 16S rRNA gene was performed with the extracted DNA for estimation of prokaryotic population in the seawater samples. The V3-V4 region of the 16S rRNA gene was targeted with the 319f (5′-ACTCCTACGGGAGGCAGCAG-3′) - 806r (5′-GGACTACHVGGGTWTCTAAT-3′) degenerate primer pair (Fadrosh et al., 2014). All qPCR reactions were performed with a CFX96 Real-time PCR System (BioRad, Hercules, CA, USA) using SYBR-Green detection chemistry (Jizhenbio, Shanghai, China). The calibration curve was constructed with a serial dilution series of 16S rRNA gene PCR fragments amplified from DNA isolated from a seawater sample and inserted in PCR2.1® vectors.

2.3. Microbial community analysis and metagenomic analysis of nitrogen and phosphorus metabolism

Low-quality reads were removed from the raw sequence data using Trimmomatic v0.36 with the parameters set as follows: LEADING: 3, TRAILING: 3, SLIDINGWINDOW: 4:15, and MINLEN:70 (Bolger et al., 2014). The quality-trimmed reads were screened for putative 16S rRNA gene fragments, using the *hmmsearch*-based Meta-RNA 3 software, with the parameters *molecule type* and *e-value* set to "*ssu*" and "1E-10", respectively (Huang et al., 2009). These reads were reconstructed to full-length 16S rRNA gene sequences using EMERGE through 100 iterations with Silva SSU database release 132 as reference (Miller et al., 2011). A QIIME-compatible OTU table was constructed with these full-length 16S rRNA gene sequences and the relative abundances of the OTUs were computed using an in-house python script, which converted the normalized coverage of each EMIRGE-synthesized 16S rRNA gene to an OTU count. The OTUs were assigned taxonomic classification using

RDP classifier v2.10.2 with Silva SSU database 132 as the reference dataset and the parameter *min_confidence* set to 0.8. The OTUs assigned to chloroplasts were removed for the downstream analysis (Caporaso et al., 2010).

For metagenomic analysis of the functional genes relevant to nitrogen- and phosphorus-metabolism, the quality-trimmed sequence reads were assembled *de novo* using metaSPAdes v3.14.0 with the parameters set to default values, and gene-coding sequences in the contigs were predicted using Prodigal v2.6.3 (Hyatt et al., 2010; Nurk et al., 2017). The predicted coding sequences were assigned functional and taxonomic annotations using DIAMOND v0.9.31.132 with NCBI's non-redundant protein database (accessed on 1/2/2020) and the Uniref90 database (accessed on 4/9/2020) as reference and the parameters set to default values (Hyatt et al., 2010). For each gene-coding sequence, only the hit that returned the highest score was taken for downstream analyses. GhostKOALA (https://www.kegg.jp/ghostkoala/) assigned KEGG Orthology (KO) numbers to the gene-coding sequences (Kanehisa et al., 2016). For annotation of carbohydrate-active enzymes (CAZymes), the predicted gene-coding sequences were searched against dbCAN HMMdb release 9.0 using the *hmmscan* command in HMMER v3.1b2 (Huang et al., 2018). Assembled contigs from the individual samples were pooled together, and for each sample, quality-trimmed raw sequence reads were mapped onto these contigs using the BWA mem v0.7.17 software (default parameters) (Li, 2013). Read counts were performed using HTSeq v0.12.4 (Anders et al., 2015). The raw counts of the coding sequences were normalized with the nucleotide length (in kilobases) and the total read count of the sample analyzed (in million reads), yielding gene coverage values in RPKM (reads per kilobase per million mapped reads).

2.4. Statistical analysis

Statistical analyses in this study were performed using nonparametric methods, due to the small sample size ($n \leq 8$). All statistical analyses were performed using R v4.0.2 (R Core Team, 2013). Pairwise comparisons of the environmental parameters between sampling sites were statistically evaluated with Student's *t*-test using *wilcox.test* function implemented in the "stats" package. Spearman's rank correlation tests were performed to evaluate statistical significance of pairwise correlations between the environmental parameters. Mantel tests evaluated pairwise correlations among physicochemical parameter matrices, the algal biomass data, the microbial community profiles, the KEGG Orthology (KO) number-based functional gene abundance profiles, and the CAZymes profiles. The dissimilarity matrices for these datasets were constructed using either Bray-Curtis dissimilatory metrics (*vegdist* function in "vegan" package) or Euclidean distance metrics (*dist* function in "stats" package), and these dissimilarity matrices were used as the inputs for the Mantel tests performed using the *mantel* function implemented in "vegan" package, with the 'correlation method' and 'permutation' options set to *spearman* and *9999*, respectively.

The non-metric multidimensional scaling (NMDS) analyses of microbial communities and functional gene compositions were performed based on the Bray-Curtis dissimilarity matrices constructed using *metaMDS* function embedded in "vegan" package. The co-occurrence networks were constructed based on the pairwise Spearman's correlation analyses performed with the relative abundances of the selected OTUs, using *cor.test* function in "stats" package. Co-occurrence networks visualizing the connections between the OTUs exhibiting significant correlations ($p<0.05$) were constructed using Cytoscape v3.7.2 (Su et al., 2014).

3. Results and discussion

3.1. Characterization of the sampling sites

Notable differences were observed between the physicochemical characteristics of the surface water samples collected from the Pingtan Sea (PIN1-PIN5) and the Xiamen Bay (XIA1-XIA3) (Fig. S1, Table S1). The surface water temperature was higher at the Xiamen Bay sites by approximately 3°C at the time of sampling, and the pH and salinity were slightly but significantly higher ($p<0.05$) at the Pingtan Sea sites. The dissolved oxygen (DO) concentration of the surface water ranged between 4.7 and 6.9 mg/L, but no significant difference was found between the two regions ($p>0.05$). The measured oxidation reduction potential (ORP) values were 43.9±2.5 mV and 22.1±6.5 mV at the Pingtan Sea and the Xiamen Bay sites, respectively (Fig. S1). Overall, Xiamen Bay was more nutrient-rich than the Pingtan Sea. The dissolved inorganic nitrogen (DIN) concentration was significantly higher ($p<0.05$) in the Xiamen Bay samples (1.5±0.3 mg-N/L) than in the Pingtan Sea samples (0.76±0.2 mg-N/L). The NO_3^- and NO_2^- concentrations were both significantly higher ($p<0.05$) in Xiamen Bay with 1.1±0.2 mg NO_3^--N/L and 0.070±0.020 mg NO_2^--N/L, as compared to 0.53±0.08 mg-NO_3^--N/L and 0.010±0.001 mg NO_2^--N/L measured in Pingtan Sea. NH_4^+ concentrations were not significantly different ($p>0.05$) between Xiamen Bay (0.31±0.11 mg NH_4^+-N /L) and Pingtan Sea (0.23±0.10 mg NH_4^+-N /L) (Fig S1). The concentrations of soluble reactive phosphorus (SRP), dissolved total phosphorus (DTP), and total phosphorus (TP) were all significantly higher in Xiamen Bay than Pingtan Sea (Fig. S1). Depletion of SRP was particularly notable in the surface seawater of the Pingtan Sea, as the SRP concentrations measured at the Pingtan Sea sites were 26±18% of the concentrations measured at the Xiamen Bay sites. The DTN-to-DTP ratio was significantly higher ($p<0.05$) in Pingtan Sea.

According to the criterion based on the Carlson's Trophic Indices (TSI), three of the five sampling locations in Pingtan Sea (PIN1, PIN4, and PIN5) and two of three in Xiamen Bay (XIA1 and XIA2) were classified as eutrophic (TSI>50). The total eukaryotic algal cell count was the highest at PIN4 (1.2×10^6 cells/L), and the algal cells morphologically identified as *Prorocentrum* spp. accounted for 91.0% of the total algal population (Table S2). The only other site with a substantial *Prorocentrum* spp. population was PIN5, where 3.6×10^5 cells/L, out of the total algal population of 5.2×10^5 cells/L, were identified as *Prorocentrum* spp. The total 16S rRNA gene copy numbers, as an indicator of prokaryotic population, ranged between 9.9±1.3 × 10^7 and 4.2±0.2 × 10^8 copies/L in Pingtan Sea and between 9.1±0.9 × 10^7 and 2.9±0.9 × 10^8 copies/L in Xiamen Bay (Fig 1b and Table S2).

3.2. Analysis of prokaryotic community and core microbiome designation

Analysis of the prokaryotic community structures of PIN1-5 and XIA1-3 identified *Proteobacteria* as the dominant phylum, with its relative abundance ranging from 76.4% to 88.2% (Fig. 2a). *Alphaproteobacteria* and *Gammaproteobacteria* constituted 18.0 - 34.6% and 41.5 - 70.0% of the prokaryotic communities, respectively. *Bacteroidia* were also abundant, constituting 6.3-17.0% of the total prokaryotic community. Although archaeal OTUs affiliated to *Thermoplasmata* and *Nitrososphaeria* were found in the metagenomes, the cumulative relative abundance of the archaeal OTUs was below 1.5% in any of the samples analyzed. The beta diversity analysis of the sea surface microbiomes clearly set the Pingtan sites apart from the Xiamen sites (Fig. 2c-e). The non-metric multidimension scaling (NMDS) plots constructed via taxonomic grouping of 16S rRNA gene sequences and functional assignments of translated enzyme sequences to KEGG Orthology (KO) groups and CAZymes groups invariably separated PIN1-5 from XIA1-3 (Fig. 2c-e), suggesting disparities between the microbiomes of these two regions, in terms of both taxonomic and functional make-ups.

The pairwise Mantel tests identified significant correlations between the taxonomic and functional compositions of the microbiomes and the states of the surface seawater at the Pingtan and Xiamen sites (Fig. 2b). Significant correlation was observed between algal biomass and 16S rRNA-based community composition (r_m=0.39, p=0.04). Algal biomass was also significantly correlated with the functional profiles of the

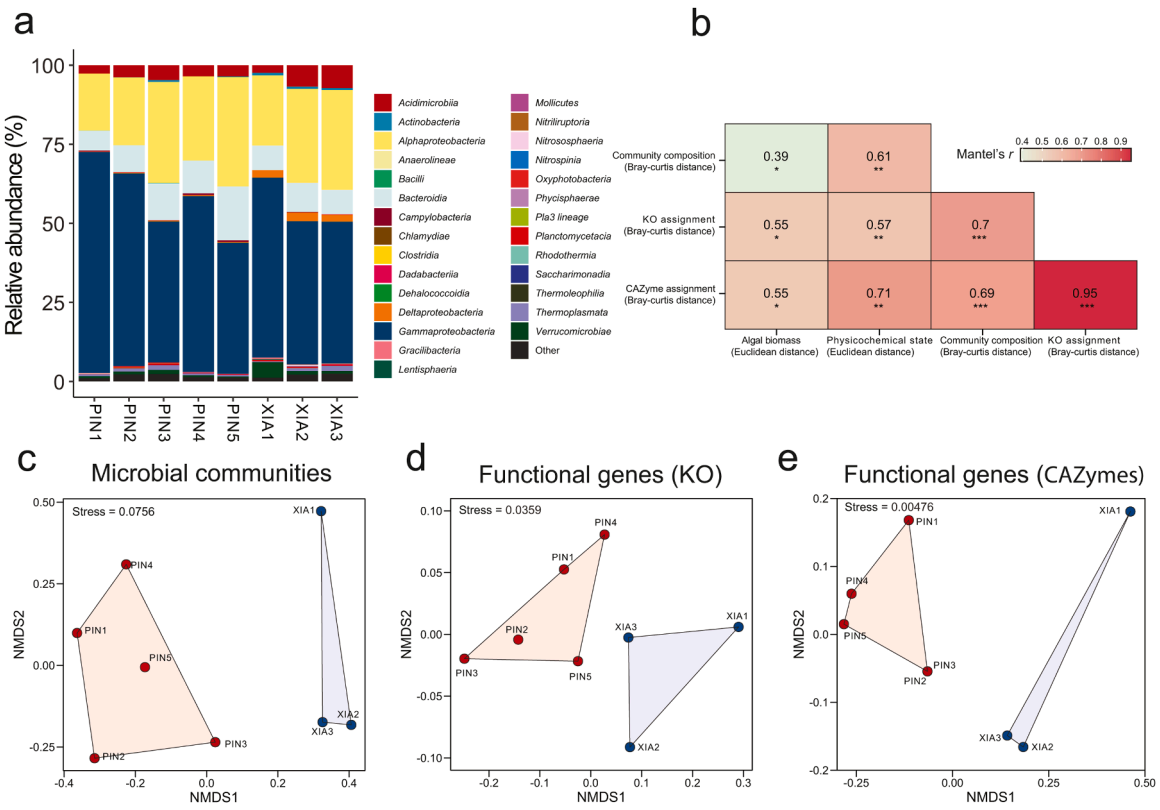

Fig. 2. Comparative analyses of the microbial community compositions of the seawater samples collected from Pingtan Sea and Xiamen Bay. (a) Microbial community compositions of the Pingtan Sea (PIN1-5) and Xiamen Bay (XIA1-3) surface water samples according to class-level taxonomic classification. (b) Pairwise correlations among the taxonomic and functional (KO and CAZyme assignments) compositions, physicochemical state, and algal biomass, as evaluated with Mantel tests. The numbers in the boxes are Mantel's *r* values indicative of the strength of the correlations, and the asterisk marks denote the significance level of the pairwise correlations (*: $p < 0.05$, **: $p < 0.01$, ***: $p < 0.001$). The NMDS plots constructed with the Bray-Curtis dissimilarity matrices computed from (c) the 16S rRNA-based community compositions and (d) the KO number-based and (e) CAZymes-based functional compositions.

microbiomes (r_m=0.55, p=0.03 and r_m=0.55, p=0.03 for correlations with KO-based and CAZyme-based functional profiles, respectively). A stronger statistically significant correlation was observed between the physicochemical states of the seawater and the prokaryotic community compositions (r_m=0.61, p=0.002) and the KO-based and CAZyme-based functional profiles (r_m=0.57, p=0.001 and r_m=0.71, p=0.002, respectively) of the microbiomes. The physicochemical states were not significantly correlated with the algal biomass (r_m=0.35, p=0.093), suggesting that a snapshot of the physicochemical state of seawater is not sufficient as an indicator for HAB. Possibly, the significant correlation between the microbiome composition and the algal biomass may imply that the history of the recent biogeochemical events, missing in a snapshot characterization of physicochemical properties, is ingrained in the taxonomic and functional compositions of the microbiome (Luria et al., 2016). Another possible scenario that can be inferred from the Mantel test results is the microbiota shaped by environmental pressure playing a direct role in algal bloom development, in a sense analogous to the key principle underlying diet-microbiome-host interactions in human and animal guts (Bindels et al., 2015).

The OTUs identified in the samples were assigned to 379 bacterial and 5 archaeal taxa (according to genus-level classification), and 47 of these taxa, shared by all 8 metagenomes, were further considered as the members of the core microbiome (Table S3). The core microbiome consisted of 46 bacterial taxa and one archaeal taxon, most of which are uncultured and understudied. The members of the core microbiome constituted vast majority of the total prokaryotic community in each of the analyzed samples, such that their cumulative relative abundance ranged between 70.4 and 76.9% at the Pingtan Sea sites and between 62.6 and 73.6% at the Xiamen Bay sites (Table S3). The core microbiome taxa with >1% relative abundance at all sites included the SAR11 clade, *Pseudoalteromonas, Vibrio, Candidatus* Actinomarina, the NS5 marine group, and an unidentified genus of *Rhodobacteraceae*. The high abundance of *Vibrio* spp. at PIN1, PIN4, PIN5, and XIA1 was especially notable. *Vibrio* spp. constituted 15.2%, 32.7%, 9.9%, and 19.3% of the prokaryotic populations at the respective sites, all of which were categorized as eutrophic according to their TSI values (>50). The relative abundance of the *Vibrio* was <4.5% at the other four sites, where, with sole exception of XIA2, the TSI values indicated mesotrophic conditions. Another core microbiome taxon affiliated to the *Vibrionaceae* family (unassignable to any distinct genus) was found at PIN2 and PIN3 sites with >10% relative abundance; however, its low abundance in PIN4 (1.3%) suggests relevance of this taxon to eutrophication or algal bloom unlikely.

3.3. Metagenomic analysis of nitrogen and phosphorus metabolism

The metagenomic profiles of nitrogen metabolism-related genes in the microbiomes suggest possible involvement of the prokaryotic microbiome in altering the availability of labile nitrogen to *Prorocentrum*-dominated algal populations (Fig. 3 and Table S4). Apart from the genes involved with urea uptake and mineralization (*ureABC* and *urtABCDE*), all of the most abundant nitrogen functional genes were relevant to dissimilatory and assimilatory NO_3^--to-NO_2^- reduction (*napAB* and *nasA*) and dissimilatory nitrite reduction to ammonium (DNRA; *nrfA* and *nirB*). The genes encoding for the periplasmic nitrate reductase, *napAB*, had substantially higher relative abundance at the Pingtan Sea sites (10.2-39.8 RPKM for *napA* and 6.0-27.3 RPKM for *napB*) than in the Xiamen Bay sites (6.9-17.1 RPKM for *napA* and 8.0-

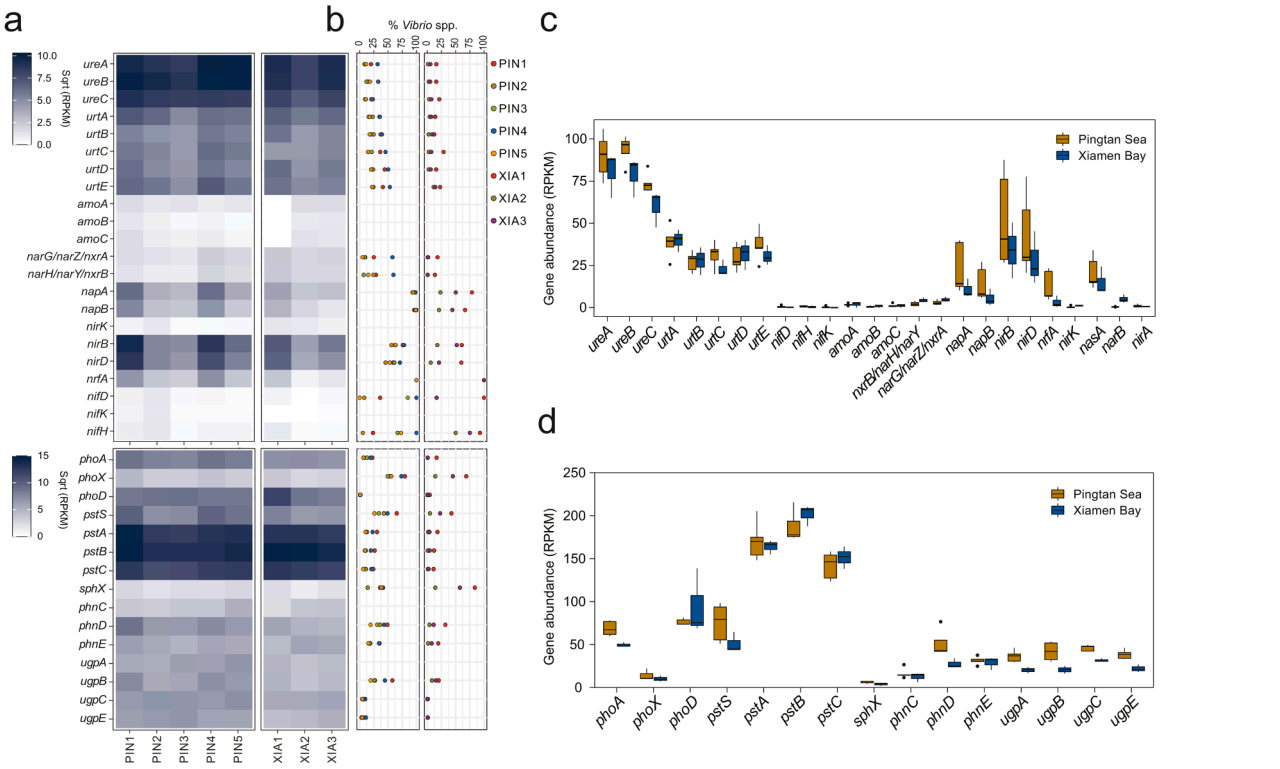

Fig. 3. Compilation of the nitrogen- or phosphorus-related functional genes recovered from the metagenomes of the Pingtan Sea and Xiamen Bay microbiomes. (a) The relative abundances of the nitrogen- and phosphorus-related functional genes are presented along with (b) the shares of these functional genes taxonomically assigned to *Vibrio* spp. (c-d) Quantitative comparisons of (c) nitrogen- and (d) phosphorus-related genes in the Pingtan Sea and Xiamen Bay microbiomes

14.2 RPKM for *napB*), although the differences were not statistically significant ($p>0.05$). The *nirB* and *nrfA* genes, encoding the catalytic subunits of the two distinct forms of nitrite reductases central to the DNRA pathway, showed high relative abundance at the Pingtan Sea and Xiamen Bay sites (Heo et al., 2020). The relative abundance of *nirB* ranged between 26.6 and 87.5 RPKM in the Pingtan Sea metagenomes, and 17.5 and 50.4 RPKM in the Xiamen Bay metagenomes. The *nrfA* genes, recovered in lower abundance than *nirB* in all metagenomes, were also substantially more abundant in the Pingtan Sea metagenomes (12.7±8.9 RPKM) than in Xiamen Bay metagenomes (3.1±3.5 RPKM) although the differences were not significant due to the large sample-to-sample variations.

Disproportionately large shares of *napA, nirB,* and *nrfA* genes were phylogenetically affiliated with *Vibrio* spp., considering that the relative abundance of *Vibrio* spp. did not exceed 33% of the total prokaryotic population according to the 16S rRNA-based community composition analyses. At the Pingtan Sea sites where this tendency was more pronounced, >93.2%, >95.8% and >56.1% of the reads mapped onto *napA, napB*, and *nirB*, respectively, were phylogenetically affiliated with the genus *Vibrio*. The gene-coding sequences identified as *nrfA* were invariably phylogenetically affiliated with *Vibrio* spp. in all metagenomes, and the relative abundance of *Vibrio* spp. exhibited significant correlation with that of *nrfA* ($p<0.05$ according to the Spearman's rank correlation). That the pronounced biases observed with regards to affiliation of *napA, napB*, and *nirB* to *Vibrio* spp. and higher relative abundance of *nrfA* observed in the Pingtan Sea microbiomes may have been due merely to the higher relative abundance of *Vibrio* spp. is possible, but unlikely. The XIA1 sample, with the highest 16S rRNA-based *Vibrio* relative abundance among the samples collected from Xiamen Bay, had lower proportions of *napA, napB*, and *nirB* genes affiliated to *Vibrio* spp. than PIN2 and PIN3 samples with 8.5- and 7.2-fold lower 16S rRNA-based *Vibrio* relative abundance. In the same context, the relative abundance of *nrfA* in the XIA1 sample (7.1 RPKM) was similar to those of the PIN2 (6.8 RPKM) and PIN3 (4.9 RPKM) samples. The nitrite reductases encoded by *nirB* have an alternate role as assimilatory nitrite reductases; however, the periplasmic nitrate reductases (NapAB) and the NrfA-type nitrite reductases have been predominantly associated with anaerobic respiratory NO_3^--to-NO_2^- and NO_2^--to-NH_4^+ reductions, respectively (Cruz-García et al., 2007; Malm et al., 2009). Thus, presence of selection pressure for *Vibrio* spp. possessing the DNRA-related functional genes was highly probable in the Pingtan Sea region.

Compared to the functional genes involved with NO_3^--to-NO_2^- reduction and DNRA, the functional genes encoding key enzymes for nitrification and denitrification were, in general, recovered in relatively low abundance (Fig. 3c). The gene abundance of *amoA* was below 3.1 RPKM in all metagenomes (1.8±0.7 and 1.9±1.7 RPKM at the Pingtan Sea and Xiamen Bay sites, respectively), and all recovered *amoA* sequences were affiliated with ammonia oxidizing archaea (AOA) of the *Candidatus* genus *Nitrosomarinus*. Despite relatively high NH_4^+-N concentrations measured at the Pingtan and Xiamen Bay sites (0.23±0.10 and 0.31±0.11 mg/L, respectively), no bacterial *amoA* was recovered in any of the metagenomes. The collective relative abundance of *nxrB, narG*, and *narZ* were 5.1±2.7 and 9.1±2.8 RPKM at the Pingtan Sea and Xiamen Bay sites, respectively. No *nirS* gene, encoding cytochrome cd_1 nitrite reductase, was found in any metagenome, and the relative abundance of *nirK* genes, encoding the copper-dependent nitrite reductases, was below 1.5 RPKM. Notably, the *nrfA*-to-*nirK* and *nirB*-to-*nirK* ratios were significantly higher in the Pingtan Sea metagenomes (80.1±68.0 and 352.5±291.2, respectively) than in the Xiamen Bay metagenomes (2.6±2.2 and 34.4±19.8, respectively), and the PIN4 site, with by far the highest algal biomass, exhibited the highest *nrfA*-to-*nirK* and *nirB*-to-*nirK* ratio (163.1 and 532.3, respectively). This selective enrichment of *nrfA* and *nirB* in the Pingtan Sea metagenomes appear too heavily biased to be solely attributable to the high relative abundance of *Vibrio* spp. (12.5±12.5%, versus 5.8±9.1% of Xiamen Bay

metagenomes). None of the signature genes for nitrogen fixation (*nifDHK*) or anammox (*hzs* and *hdh*) was recovered at a significant abundance (<1.7 RPKM).

Metagenomic interrogation of phosphorus uptake and metabolism also identified several notable differences between the Pingtan Sea and Xiamen Bay microbiomes (Fig. 3a and Fig. 3d). The *ugpABCE* genes, encoding ATP-binding cassette (ABC) transporters for uptake of glycerol-3-phosphate and glycerophocholine, were found in significantly higher relative abundance in the Pingtan Sea metagenomes than in the Xiamen Bay metagenomes. The phosphonate transporter gene *phnD* and the high-affinity phosphate binding protein *pstS*, were both also significantly more abundant in the Pingtan Sea microbiomes (51.7±15.0 RPKM and 75.5±21.6 RPKM, respectively) than in the Xiamen Bay microbiomes (27.4±5.7 RPKM and 50.9±11.8 RPKM, respectively). As these phosphorus uptake genes are known to be expressed under P_i-deficient conditions to cope for phosphorus starvation, their abundance in Pingtan Sea metagenomes was consistent with the low concentrations of soluble reactive phosphorus ($7.9\pm4.3 \times 10^{-3}$ mg/L) at the Pingtan Sea sites (Ilikchyan et al., 2009; Scanlan et al., 1997; Yang et al., 2009). Substantial proportions of *phnD* (35.5±11.5%), *pstS* (43.3±15.0%), and *ugpB* (34.8±15.8%) sequences recovered from the Pingtan Sea metagenomes were affiliated with *Vibrio* spp., suggesting that possession of these diverse means of alternative phosphorus uptake may have contributed to the disproportionate proliferation of *Vibrio* spp. observed in Pingtan Sea.

The genes encoding three distinct forms of alkaline phosphatases, *phoA, phoX*, and *phoD*, were found in all metagenomes, and *phoA* and *phoD*, both with RPKM values above 50, were among the most abundant nitrogen- or phosphorus-related functional genes in the metagenomes (Fig. 3d). The *phoA* genes were significantly more abundant in the Pingtan metagenomes (68.7±8.4 RPKM) than in the Xiamen Bay metagenomes (49.5±2.6 RPKM; $p<0.05$); however, the abundances of *phoX* and *phoD* were not significantly different between the two regions ($p>0.05$). In the Pingtan metagenomes, *Vibrio*-affiliated sequences accounted for the majority of *phoX* (62.3±13.4%), while only 13.6±7.0% and 0.8±0.5% of *phoA* and *phoD*, both at least 3.4-fold more abundant than *phoX*, were affiliated with *Vibrio* spp. Therefore, the abundances of alkaline phosphatase genes appear to have little relevance to *Vibrio* proliferation or *Prorocentrum* bloom.

3.4. Vibrio-dinoflagellate relationship as inferred from the microbial network analysis of the core microbiome

Microbial network analysis of the core microbiome further substantiated the alleged association between abundance of *Vibrio* spp. and dinoflagellate bloom (Fig. 4a). The relative abundances of two core microbiome taxa, including *Pseudoalteromonas* and an unidentified genus of the family *Cryomorphaceae*, showed significant positive correlation with the algal biomass, and the relative abundances of four other core microbiome taxa exhibited significant negative correlation (Spearman's $|r| > 0.7$, $p<0.05$; Fig. 4b). The core microbiome taxon affiliated to the genus *Vibrio* was positively but not significantly correlated with algal biomass ($r=0.26$, $p=0.53$); however, its relative abundance had strong significant positive correlation ($r=0.81$, $p=0.015$) with the relative abundance of *Pseudoalteromonas*, and significant negative correlations with those of three core microbiome taxa negatively correlated with algal biomass, including Marine Group II of the phylum *Euryarchaeota*, an unidentified genus of the family *Parvibaculaceae*, and the IS-44 subgroup of the family *Nitrosomonadaceae* ($r=-0.71$, $p=0.047$; $r=-0.71$, $p=0.047$; $r=-0.79$, $p=0.021$, respectively). Of note, co-abundance of *Pseudoalteromonas* spp. with eukaryotic algae has been previously observed and mechanistically explained with basis on the capability of the microorganisms belonging to this taxon to prey on eukaryotic algae (Skovhus et al., 2004). Alongside the observation that *Vibrio* spp. was the single most abundant taxon in the PIN4 microbiome most severely affected by HAB, these co-occurrence patterns surrounding *Vibrio* in the core microbiome network corroborate the possibility of a causal association of *Vibrio* spp. with HAB, despite the lack of statistically significant correlation between the relative abundance of the *Vibrio* and the algal biomass.

3.5. Ecological association of Vibrio spp. with dinoflagellate algal bloom

As these metagenome analyses suggest, association of *Vibrio* spp. to the *Prorocentrum*-dominated algal blooms was apparent in the examined segment of coastal East China Sea. Strong significant correlations between the abundance of *Vibrio* spp. and the environmental metrics for eutrophication (TSI; $r=0.833$, $p=0.011$) as well as the chlorophyll a concentration ($r=0.762$, $p=0.028$) also support that the *Vibrio* and algal

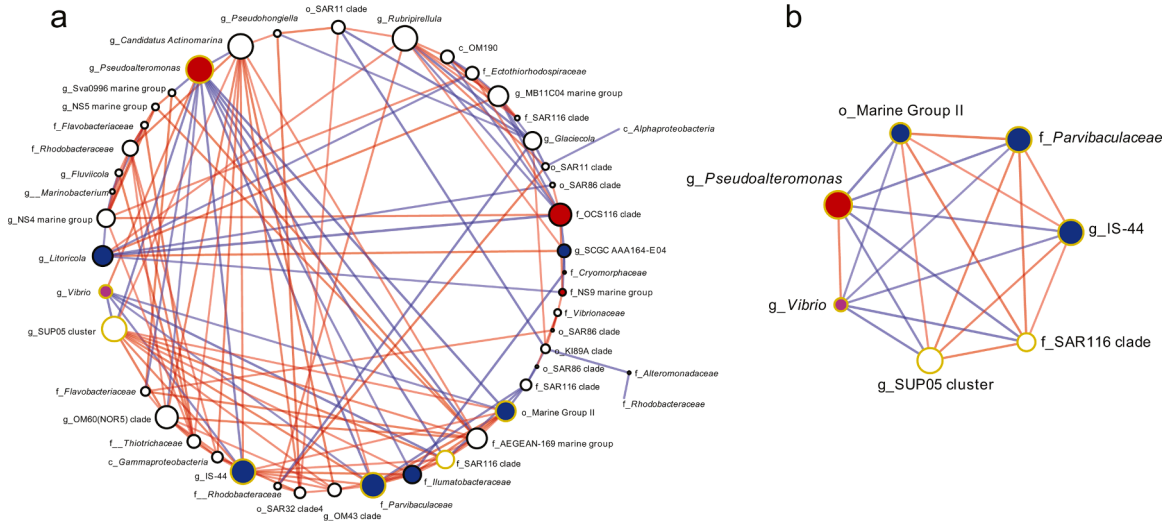

Fig. 4. Co-occurrence network analysis of the core microbiome. (a) Co-occurrence network based on the pairwise Spearman's rank correlation analyses performed with the relative abundance data of the 47 core microbiome taxa. Only statistically significant ($p<0.05$) correlations are visualized with red (positive) or blue (negative) edges, and the thickness of the edges are proportional to the magnitudes of the *r* values. The size of a node is proportional to the number of edges via which it is connected to other nodes. The colors of the nodes indicate taxa which had significantly positive (red) or negative (blue) correlation with algal biomass. (b) An abridged co-occurrence network constructed with the subset of the core microbiome taxa found to have relative abundances significantly correlated with that of the *Vibrio* genus (denoted with yellow boundary in (a)).

proliferation may be mechanistically correlated (Table S5). These observations are in line with a number of previous studies that have reported occurrences of *Vibrio* blooms in coastal seas simultaneous with blooms of phytoplanktons, e.g., cyanobacteria, diatoms, and dinoflagellates, or immediately following their demise (Asplund et al., 2011; Eiler et al., 2006; Gilbert et al., 2012; Main et al., 2015; Takemura et al., 2014). In a study that monitored microbial population dynamics over a six-year period off the coast of Plymouth, UK, the time point at which a single *Vibrio* sp. dominated the prokaryotic population, representing 54% of the entire pool of 16S rRNA sequences, coincided with a peak in the population of a diatom species *Chaetoceros compressus* (Gilbert et al., 2012). Another study performed during raphidophyte blooms in Delaware's inland bays identified significant correlation between the abundances of particle-associated *Vibrio* spp. and the raphidophyte population (Main et al., 2015).

These previous studies have hypothetically attributed the observed abundance of *Vibrio* spp. to the benefits these opportunistic fast-growing bacteria may gain from phytoplanktons, such as protection from zooplankton predation and provision of algal exudates or detritus as organic substrates (Asplund et al., 2011; Main et al., 2015; Takemura et al., 2014). Although *Vibrio* spp. may form biofilms attached to microalgal cells and detritus, physically and chemically protected from grazing, recent culture-independent studies have repeatedly identified particle-associated fractions as minor fractions of *Vibrio* population in seawater (Liang et al., 2019). Thus, supply of labile organics, photosynthetically produced and released by algal counterparts, is deemed more likely as the primary mechanism via which algal blooms accommodate disproportionate proliferation of *Vibrio* spp. (Thickman and Gobler, 2017). Further, several *Vibrio* species have been physiologically characterized as alginolytic, and thus may be able to utilize dead algal biomass or even be algicidal. In this study, core microbiome analysis identified a strong significant positive correlation between *Vibrio* and *Pseudoalteromonas*, a taxon widely-known to include algicidal bacteria (Lee et al., 2000). This correlation may be interpreted as two groups of specialists sharing a habitat abound with their common substrates, i.e., live or dead algal biomass and/or algae-derived organic materials. It may also be possible that smaller organic compounds produced from *Pseudoalteromanas*-mediated algal biomass digestion may serve as more labile organic substrates for fast-growing *Vibrio* spp. (Thickman and Gobler, 2017). Either hypothesized mechanism would be consistent with the co-occurrence of *Vibrio* proliferation and *Prorocentrum*-dominant algal bloom observed in this study.

Whether the presumed *Vibrio-Prorocentrum* association may be a commensal relationship, benefitting only *Vibrio* spp., or a mutually-beneficial symbiotic relationship, cannot be inferred from these previous reports, as none of them investigated or discussed how *Vibrio* spp. may contribute to algal blooms. Nevertheless, the findings from the comparative metagenomic analysis of the nitrogen functional genes suggest scenarios how *Vibrio* proliferation may provide positive feedback to growth of *Prorocentrum* spp. and possibly other eukaryotic microalgae. The proportion of *Vibrio*-associated functional genes were, in general, higher at the Pingtan Sea sites than at the Xiamen Bay sites, probably due merely to the higher *Vibrio* abundance; however, *Vibrio*'s exclusive ownership of DNRA-related functional genes, i.e., *napAB* and *nrfA*, and the near complete absence of denitrification-related functional genes (*nirK* and *nirS*) that are often found in genomes of marine heterotrophic bacteria (e.g., algicidal *Pseudoalteromonas* spp.) are not explicable merely with the high *Vibrio* abundance. The DO concentrations of the bulk seawater at the Pingtan Sea sites, including the PIN4 site with the highest *Prorocentrum* population and algal biomass, indicated that the bulk seawater was oxic at the time of sampling, which, due to logistical reasons, took place during the daytime. Under oxic conditions, DNRA is not likely to occur, as it is known as a strictly anaerobic process; however considering the high populations of the fast-metabolizing *Vibrio* and *Prorocentrum* that may be potent O_2 sinks at dark hours, it is plausible that periodic oxic-anoxic shifts may occur in the region, especially at highly eutrophicated locales such as the PIN4 and PIN5 sites (Broman et al., 2021; Hitchcock et al., 2014). Spatial microaerobic or anoxic niches may also exist, such as in biofilms attached to particle surfaces, microbial aggregates, and intracellular spaces within zooplankton or phytoplankton where *Vibrio* spp. may be able to colonize (Bianchi et al., 2018; Broman et al., 2021; Espinoza-Vergara et al., 2020; Van der Henst et al., 2016). Rapid decay of algal carcass, and/or upwelling of hypoxic bottom water may also cause temporal anoxia that may not be captured by snapshots of DO measurement (Lee et al., 2005; Pitcher et al., 2014). Further, the redox potentials measured *in situ* at the Pingtan Sea (43.9±2.5 mV) sites were in fact, substantially lower than the standard redox potentials (at pH 7.0) of NO_3^--to-NO_2^- (420 mV) and NO_2^--to-NH_4^+ reduction (440 mV), despite the DO concentrations ranging between 4.73 – 6.89 mg L^{-1}. Thus, it is highly likely that at least some of the *napAB*- and *nrfA*-possessing *Vibrio* spp. become DNRA-active once initial patchy *Prorocentrum* blooms, supported by initially available dissolved NH_4^+-N, start to develop. The *Vibrio*-mediated DNRA may promote growth of *Prorocentrum* spp. by providing additional supply of NH_4^+, generally known as a more efficient nitrogen source for fast-growing dinoflagellates than NO_3^-, as a positive feedback, bringing about an increase in the area and intensity of HAB (Ou et al., 2019). Although any decisive conclusion cannot be reached solely based on the metagenome analysis, the findings from this study are certainly compelling indications that NH_4^+-production via DNRA may be key to the hypothesized symbiotic association between *Vibrio* spp. and *Prorocentrum* spp. and warrant further attention to the role that DNRA may play in *Prorocentrum*-dominated HAB.

4. Conclusions

Occurrences of severe marine algal blooms are often attributed to nitrogen and/or phosphorus enrichment relieving nutrient limitations to algal growth; however conclusive evidence of the presumed correlation between the nutrient conditions and algal population has remained elusive. In this study, we attempted a different avenue of approach, using comparative metagenomics to investigate any association between surface seawater microbiomes and *Prorocentrum*-dominated algal blooms in East China Sea. The most prominent feature that distinguished the microbiomes of Pingtan Sea with frequent severe *Prorocentrum* blooms from that of Xiamen Bay much less frequently affected was enrichment of organisms affiliated with *Vibrio* spp. and disproportionately biased affiliation of *napAB* and *nrfA* to this taxon. The alleged association between DNRA-capable *Vibrio* spp. and algal bloom in this locale was further substantiated via core microbiome network analysis. The findings suggest a previously unidentified causal association between *Vibrio* proliferation and dinoflagellate bloom in subtropical marine environment and broach the possibility that DNRA may play a key role in mutually beneficial symbiosis between the two groups of organisms.

Declaration of Competing Interest

The authors declare that they have no known competing financial interests or personal relationships that could have appeared to influence the work reported in this paper.

Authors statement

DDK and LW contributed equally for the preparation of the manuscript. XC, YZ, CS, and SY designed the experiments. LW, XC, YZ, and CS collected seawater samples and performed on-site experiments. LW, DK, and DG performed laboratory experiments, including DNA extraction and library preparation. DDK and SY performed statistical and metagenomic analyses. DDK, LW, XC, YZ, CS, and SY drafted the manuscript.

Acknowledgements

The authors would like to thank Prof. Bongkeun Song (Virginia Institute of Marine Science, USA) for kindly reviewing the manuscript and providing invaluable suggestions. This work was financially supported by grants from the National Key Research and Development Program of China (2016YFE0202100) and Natural Science Foundation of China (41611540341, 41877381), and internal funding from the State Key Laboratory of Freshwater Ecology and Biotechnology (2019FBZ01).

Supplementary materials

Supplementary material associated with this article can be found, in the online version, at doi:10.1016/j.watres.2021.117625.

References

Anders, S., Pyl, P.T., Huber, W., 2015. HTSeq-a Python framework to work with high-throughput sequencing data. Bioinformatics 31 (2), 166–169.
Anderson, D.M., Cembella, A.D., Hallegraeff, G.M, 2012. Progress in understanding harmful algal blooms: paradigm shifts and new technologies for research, monitoring, and management. Annu. Rev. Mar. Sci. 4, 143–176.
Asplund, M.E., Rehnstam-Holm, A.S., Atnur, V., Raghunath, P., Saravanan, V., Härnström, K., Collin, B., Karunasagar, I., Godhe, A., 2011. Water column dynamics of *Vibrio* in relation to phytoplankton community composition and environmental conditions in a tropical coastal area. Environ. Microbiol. 13 (10), 2738–2751.
Azanza, R.V., Fukuyo, Y., Yap, L.G., Takayama, H., 2005. *Prorocentrum minimum* bloom and its possible link to a massive fish kill in Bolinao, Pangasinan, Northern Philippines. Harmful Algae 4 (3), 519–524.
Ben-Gharbia, H., Yahia, O.K.-D., Amzil, Z., Chomérat, N., Abadie, E., Masseret, E., Sibat, M., Zmerli Triki, H., Nouri, H., Laabir, M., 2016. Toxicity and growth assessments of three thermophilic benthic dinoflagellates (*Ostreopsis* cf. *ovata*, *Prorocentrum lima* and *Coolia monotis*) developing in the Southern Mediterranean Basin. Toxins 8 (10), 297.
Bianchi, D., Weber, T.S., Kiko, R., Deutsch, C., 2018. Global niche of marine anaerobic metabolisms expanded by particle microenvironments. Nat. Geosci. 11 (4), 263–268.
Bindels, L.B., Delzenne, N.M., Cani, P.D., Walter, J., 2015. Towards a more comprehensive concept for prebiotics. Nat. Rev. Gastro. Hepat. 12 (5), 303.
Bolger, A.M., Lohse, M., Usadel, B., 2014. Trimmomatic: a flexible trimmer for Illumina sequence data. Bioinformatics 30 (15), 2114–2120.
Broman, E., Zilius, M., Samuiloviene, A., Vybernaite-Lubiene, I., Politi, T., Klawonn, I., Voss, M., Nascimento, F.J., Bonaglia, S., 2021. Active DNRA and denitrification in oxic hypereutrophic waters. Water Res 194, 116954.
Caporaso, J.G., Kuczynski, J., Stombaugh, J., Bittinger, K., Bushman, F.D., Costello, E.K., Fierer, N., Pena, A.G., Goodrich, J.K., Gordon, J.I, 2010. QIIME allows analysis of high-throughput community sequencing data. Nat. Methods 7 (5), 335–336.
Carlson, R.E., 1977. A trophic state index for lakes. Limnol. Oceanogr. 22 (2), 361–369.
Chin, J.P., Quinn, J.P., McGrath, J.W, 2018. Phosphate insensitive aminophosphonate mineralisation within oceanic nutrient cycles. ISME J 12 (4), 973–980.
Conley, D.J., Carstensen, J., Aigars, J., Axe, P., Bonsdorff, E., Eremina, T., Haahti, B.M., Humborg, C., Jonsson, P., Kotta, J., 2011. Hypoxia is increasing in the coastal zone of the Baltic Sea. Environ. Sci. Technol. 45 (16), 6777–6783.
Cruz-García, C., Murray, A.E., Klappenbach, J.A., Stewart, V., Tiedje, J.M., 2007. Respiratory nitrate ammonification by *Shewanella oneidensis* MR-1. J. Bacteriol. 189 (2), 656–662.
Dore, J.E., Karl, D.M, 1996. Nitrification in the euphotic zone as a source for nitrite, nitrate, and nitrous oxide at Station ALOHA. Limnol. Oceanogr. 41 (8), 1619–1628.
Edler, L., 1979. Recommendations for marine biological studies in the Baltic Sea: phytoplankton and chlorophyll. Baltic Mar. Biol. 5, 1–38.
Eiler, A., Johansson, M., Bertilsson, S., 2006. Environmental influences on *Vibrio* populations in northern temperate and boreal coastal waters (Baltic and Skagerrak Seas). Appl. Environ. Microb. 72 (9), 6004–6011.
Espinoza-Vergara, G., Hoque, M.M., McDougald, D., Noorian, P., 2020. The impact of protozoan predation on the pathogenicity of *Vibrio cholerae*. Front. Microbiol. 11, 17.
Fadrosh, D.W., Ma, B., Gajer, P., Sengamalay, N., Ott, S., Brotman, R.M., Ravel, J., 2014. An improved dual-indexing approach for multiplexed 16S rRNA gene sequencing on the Illumina MiSeq platform. Microbiome 2 (1), 1–7.
Fan, C., Glibert, P.M., Burkholder, J.M, 2003. Characterization of the affinity for nitrogen, uptake kinetics, and environmental relationships for *Prorocentrum minimum* in natural blooms and laboratory cultures. Harmful Algae 2 (4), 283–299.
Gallegos, C.L., Bergstrom, P.W, 2005. Effects of a *Prorocentrum minimum* bloom on light availability for and potential impacts on submersed aquatic vegetation in upper Chesapeake Bay. Harmful Algae 4 (3), 553–574.
Gilbert, J.A., Steele, J.A., Caporaso, J.G., Steinbrück, L., Reeder, J., Temperton, B., Huse, S., McHardy, A.C., Knight, R., Joint, I., 2012. Defining seasonal marine microbial community dynamics. ISME J. 6 (2), 298–308.
Glibert, P.M., Mayorga, E., Seitzinger, S., 2008. *Prorocentrum minimum* tracks anthropogenic nitrogen and phosphorus inputs on a global basis: application of spatially explicit nutrient export models. Harmful Algae 8 (1), 33–38.
Greenberg, A.E., Clesceri, L.S., Eaton, A.D, 2012. Standard methods for the examination of water and wastewater, 22nd. American Public Health Association, Washington.
Griffith, G.W., Ozkose, E., Theodorou, M.K., Davies, D.R, 2009. Diversity of anaerobic fungal populations in cattle revealed by selective enrichment culture using different carbon sources. Fungal Ecol. 2 (2), 87–97.
Heil, C.A., Glibert, P.M., Fan, C., 2005. *Prorocentrum minimum* (Pavillard) Schiller: a review of a harmful algal bloom species of growing worldwide importance. Harmful Algae 4 (3), 449–470.
Heo, H., Kwon, M., Song, B., Yoon, S., 2020. Involvement of NO_3^- in ecophysiological regulation of dissimilatory nitrate/nitrite reduction to ammonium (DNRA) is implied by physiological characterization of soil DNRA bacteria isolated via a colorimetric screening method. Appl. Environ. Microbiol. 86 (17) e01054-01020.
Hitchcock, G.L., Kirkpatrick, G., Lane, P.V., Langdon, C., 2014. Comparative diel oxygen cycles preceding and during a Karenia bloom in Sarasota Bay, Florida, USA. Harmful Algae 38, 95–100.
Hoppe, H.G., 2003. Phosphatase activity in the sea. Hydrobiologia 493.
Huang, L., Zhang, H., Wu, P., Entwistle, S., Li, X., Yohe, T., Yi, H., Yang, Z., Yin, Y., 2018. dbCAN-seq: a database of carbohydrate-active enzyme (CAZyme) sequence and annotation. Nucleic Acids Res. 46 (D1), D516–D521.
Huang, Y., Gilna, P., Li, W., 2009. Identification of ribosomal RNA genes in metagenomic fragments. Bioinformatics 25 (10), 1338–1340.
Hyatt, D., Chen, G.L., LoCascio, P.F., Land, M.L., Larimer, F.W., Hauser, L.J, 2010. Prodigal: prokaryotic gene recognition and translation initiation site identification. BMC Bioinformatics 11 (1), 1–11.
Ilikchyan, I.N., McKay, R.M.L., Zehr, J.P., Dyhrman, S.T., Bullerjahn, G.S, 2009. Detection and expression of the phosphonate transporter gene *phnD* in marine and freshwater picocyanobacteria. Environ. Microbiol. 11 (5), 1314–1324.
Kanehisa, M., Sato, Y., Morishima, K., 2016. BlastKOALA and GhostKOALA: KEGG tools for functional characterization of genome and metagenome sequences. J. Mol. Biol. 428 (4), 726–731.
Kuypers, M.M., Marchant, H.K., Kartal, B., 2018. The microbial nitrogen-cycling network. Nat. Rev. Microbiol. 16 (5), 263.
Labry, C., Delmas, D., Herbland, A., 2005. Phytoplankton and bacterial alkaline phosphatase activities in relation to phosphate and DOP availability within the Gironde plume waters (Bay of Biscay). J. Exp. Mar. Biol. Ecol. 318 (2), 213–225.
Langner, C., Hendrix, P., 1982. Evaluation of a persulfate digestion method for particulate nitrogen and phosphorus. Water Res. 16 (10), 1451–1454.
Lee, J.H.W., Hodgkiss, I.J., Wong, K., Lam, I., 2005. Real time observations of coastal algal blooms by an early warning system. Estuar. Coast. Shelf. S. 65 (1-2), 172–190.
Lee, S.-o., Kato, J., Takiguchi, N., Kuroda, A., Ikeda, T., Mitsutani, A., Ohtake, H., 2000. Involvement of an extracellular protease in algicidal activity of the marine bacterium *Pseudoalteromonas* sp. strain A28. Appl. Environ. Microbiol. 66 (10), 4334–4339.
Li, H., 2013. Aligning sequence reads, clone sequences and assembly contigs with BWA-MEM. arXiv Prepr. ArXiv.
Li, J., Glibert, P.M., Zhou, M., 2010. Temporal and spatial variability in nitrogen uptake kinetics during harmful dinoflagellate blooms in the East China Sea. Harmful Algae 9 (6), 531–539.
Li, Y., Lü, S., Jiang, T., Xiao, Y., You, S., 2011. Environmental factors and seasonal dynamics of *Prorocentrum* populations in Nanji Islands National Nature Reserve, East China Sea. Harmful Algae 10 (5), 426–432.
Liang, J., Liu, J., Wang, X., Lin, H., Liu, J., Zhou, S., Sun, H., Zhang, X., 2019. Spatiotemporal dynamics of free-living and particle-associated *Vibrio* communities in the northern Chinese marginal seas. Appl. Environ. Microbiol. 85 (9), e00217–e00219.
Lu, D., Goebel, J., Qi, Y., Zou, J., Han, X., Gao, Y., Li, Y., 2005. Morphological and genetic study of *Prorocentrum donghaiense* Lu from the East China Sea, and comparison with some related *Prorocentrum* species. Harmful Algae 4 (3), 493–505.
Luo, H., Benner, R., Long, R.A., Hu, J., 2009. Subcellular localization of marine bacterial alkaline phosphatases. P. Natl. Acad. Sci. 106 (50), 21219–21223.
Luo, H., Moran, M.A, 2013. Assembly-free metagenomic analysis reveals new metabolic capabilities in surface ocean bacterioplankton. Environ. Microbiol. Rep. 5 (5), 686–696.
Luria, C.M., Amaral-Zettler, L.A., Ducklow, H.W., Rich, J.J, 2016. Seasonal succession of free-living bacterial communities in coastal waters of the Western Antarctic Peninsula. Front. Microbiol. 7, 1731.
Mahmud, M., Ejeian, F., Azadi, S., Myers, M., Pejcic, B., Abbasi, R., Razmjou, A., Asadnia, M., 2020. Recent progress in sensing nitrate, nitrite, phosphate, and ammonium in aquatic environment. Chemosphere, 127492.
Main, C.R., Salvitti, L.R., Whereat, E.B., Coyne, K.J, 2015. Community-level and species-specific associations between phytoplankton and particle-associated *Vibrio* species in Delaware's inland bays. Appl. Environ. Microbiol. 81 (17), 5703–5713.
Malm, S., Tiffert, Y., Micklinghoff, J., Schultze, S., Joost, I., Weber, I., Horst, S., Ackermann, B., Schmidt, M., Wohlleben, W., Ehlers, S., 2009. The roles of the nitrate reductase NarGHJI, the nitrite reductase NirBD and the response regulator GlnR in nitrate assimilation of *Mycobacterium tuberculosis*. Microbiology 155 (4), 1332–1339.
Michael Beman, J., Popp, B.N., Alford, S.E., 2012. Quantification of ammonia oxidation rates and ammonia-oxidizing archaea and bacteria at high resolution in the Gulf of California and eastern tropical North Pacific Ocean. Limnol. Oceanogr. 57 (3), 711–726.
Miller, C.S., Baker, B.J., Thomas, B.C., Singer, S.W., Banfield, J.F, 2011. EMIRGE: reconstruction of full-length ribosomal genes from microbial community short read sequencing data. Genome Biol. 12 (5), 1–14.
Mo, Y., Ou, L., Lin, L., Huang, B., 2020. Temporal and spatial variations of alkaline phosphatase activity related to phosphorus status of phytoplankton in the East China Sea. Sci. Tot. Environ. 731, 139192.
Murphy, J., Riley, J.P, 1962. A modified single solution method for the determination of phosphate in natural waters. Anal. Chim. Acta 27, 31–36.

Nascimento, S.M., Mendes, M.C.Q., Menezes, M., Rodríguez, F., Alves-de-Souza, C., Branco, S., Riobó, P., Franco, J., Nunes, J.M.C., Huk, M., 2017. Morphology and phylogeny of *Prorocentrum caipirignum* sp. nov.(Dinophyceae), a new tropical toxic benthic dinoflagellate. Harmful Algae 70, 73–89.

Nurk, S., Meleshko, D., Korobeynikov, A., Pevzner, P.A, 2017. metaSPAdes: a new versatile metagenomic assembler. Genome Res. 27 (5), 824–834.

Nusch, E., 1980. Comparison of different methods for chlorophyll and phaeopigment determination. Ergeb. Limnol. 14, 14–36.

Olenina, I., Hajdu, S., Edler, L., Andersson, A., Wasmund, N., Busch, S., Göbel, J., Gromisz, S., Huseby, S., Huttunen, M., Jaanus, A., Kokkonen, P., Ledaine, I., Niemkiewicz, E., 2006. Biovolumes and size-classes of phytoplankton in the Baltic Sea. Baltic Sea Environmental Proceedings 144.

Ou, L., Qin, X., Shi, X., Feng, Q., Zhang, S., Lu, S., Qi, Y., 2020. Alkaline phosphatase activities and regulation in three harmful *Prorocentrum* species from the coastal waters of the East China Sea. Microb. Ecol. 79 (2), 459–471.

Ou, L., Huang, K., Li, J., Jing, W., Dong, H., 2019. Transcriptomic responses of harmful dinoflagellate *Prorocentrum donghaiense* to nitrogen and light. Mar. Pollut. Bull. 149, 110617.

Patey, M.D., Rijkenberg, M.J., Statham, P.J., Stinchcombe, M.C., Achterberg, E.P., Mowlem, M., 2008. Determination of nitrate and phosphate in seawater at nanomolar concentrations. TrAC Trends Anal. Chem. 27 (2), 169–182.

Pitcher, G.C., Probyn, T.A., du Randt, A., Lucas, A.J., Bernard, S., Evers-King, H., Lamont, T., Hutchings, L., 2014. Dynamics of oxygen depletion in the nearshore of a coastal embayment of the southern Benguela upwelling system. J. Geophys. Res-Oceans 119 (4), 2183–2200.

R Core Team, 2013. R: A language and environment for statistical computing. R Foundation for Statistical Computing, Vienna Austria. URL https://www.R-project.org/.

Raimundo, J., Reis, C.M.G., Ribeiro, M.M, 2018. Rapid, simple and potentially universal method for DNA extraction from *Opuntia* spp. fresh cladode tissues suitable for PCR amplification. Mol. Biol. Rep. 45 (5), 1405–1412.

Scanlan, D.J., Silman, N.J., Donald, K.M., Wilson, W.H., Carr, N.G., Joint, I., Mann, N.H, 1997. An immunological approach to detect phosphate stress in populations and single cells of photosynthetic picoplankton. Appl. Environ. Microbiol. 63 (6), 2411–2420.

Sebastian, M., Ammerman, J.W, 2009. The alkaline phosphatase PhoX is more widely distributed in marine bacteria than the classical PhoA. ISME J. 3 (5), 563–572.

Shin, H.H., Li, Z., Mertens, K.N., Seo, M.H., Gu, H., Lim, W.A., Yoon, Y.H., Soh, H.Y., Matsuoka, K., 2019. *Prorocentrum shikokuense* Hada and *P. donghaiense* Lu are junior synonyms of *P. obtusidens* Schiller, but not of *P. dentatum* Stein (Prorocentrales, Dinophyceae). Harmful Algae 89, 101686.

Skovhus, T.L., Ramsing, N.B., Holmström, C., Kjelleberg, S., Dahllöf, I., 2004. Real-time quantitative PCR for assessment of abundance of *Pseudoalteromonas* species in marine samples. Appl. Environ. Microbiol. 70 (4), 2373–2382.

Su, G., Morris, J.H., Demchak, B., Bader, G.D, 2014. Biological network exploration with Cytoscape 3. Curr. Protoc. Bioinformatics 47 (1), 8.13. 11-18.13. 24.

Suzumura, M., Hashihama, F., Yamada, N., Kinouchi, S., 2012. Dissolved phosphorus pools and alkaline phosphatase activity in the euphotic zone of the western North Pacific Ocean. Front. Microbiol. 3, 99.

Takemura, A.F., Chien, D.M., Polz, M.F, 2014. Associations and dynamics of Vibrionaceae in the environment, from the genus to the population level. Front. Microbiol. 5, 38.

Tang, D., Di, B., Wei, G., Ni, I., Wang, S., 2006. Spatial, seasonal and species variations of harmful algal blooms in the South Yellow Sea and East China Sea. Hydrobiologia 568 (1), 245–253.

Thickman, J.D., Gobler, C.J, 2017. The ability of algal organic matter and surface runoff to promote the abundance of pathogenic and non-pathogenic strains of *Vibrio parahaemolyticus* in Long Island Sound, USA. PLoS. One 12 (10), e0185994.

Thomson, B., Wenley, J., Currie, K., Hepburn, C., Herndl, G.J., Baltar, F., 2019. Resolving the paradox: continuous cell-free alkaline phosphatase activity despite high phosphate concentrations. Mar. Chem. 214, 103671.

Trojánek, Z., Kovařík, A., Španová, A., Marošiová, K., Horák, D., Rittich, B., 2018. Application of magnetic polymethacrylate-based microspheres for the isolation of DNA from raw vegetables and processed foods of plant origin. J. Food Process. Pres. 42 (1), e13384.

Turner, E.L., Paudel, B., Montagna, P.A, 2015. Baseline nutrient dynamics in shallow well mixed coastal lagoon with seasonal harmful algal blooms and hypoxia formation. Mar. Pollut. Bull. 96 (1-2), 456–462.

Tyler, J.E., 1968. The secchi disc. Limnol. Oceanogr. 13 (1), 1–6.

Van der Henst, C., Scrignari, T., Maclachlan, C., Blokesch, M., 2016. An intracellular replication niche for Vibrio cholerae in the amoeba Acanthamoeba castellanii. ISME J 10 (4), 897–910.

Varkitzi, I., Pagou, K., Graneli, E., Hatzianestis, I., Pyrgaki, C., Pavlidou, A., Montesanto, B., Economou-Amilli, A., 2010. Unbalanced N: P ratios and nutrient stress controlling growth and toxin production of the harmful dinoflagellate *Prorocentrum lima* (Ehrenberg) Dodge. Harmful Algae 9 (3), 304–311.

Wankel, S.D., Kendall, C., Pennington, J.T., Chavez, F.P., Paytan, A., 2007. Nitrification in the euphotic zone as evidenced by nitrate dual isotopic composition: Observations from Monterey Bay. California. Global Biogeochem. Cycles 21 (2).

Yang, K., Wang, M., Metcalf, W.W, 2009. Uptake of glycerol-2-phosphate via the ugp-encoded transporter in *Escherichia coli* K-12. J. Bacteriol. 191 (14), 4667–4670.

Yu, R., Lü, S., Liang, Y., 2018. In: Glibert, P.M., Berdalet, E., Burford, M.A., Pitcher, G.C., Zhou, M. (Eds.), Global Ecology and Oceanography of Harmful Algal Blooms. Internet Project, 309–316.

Zhou, Y., Zhang, Y., Li, F., Tan, L., Wang, J., 2017. Nutrients structure changes impact the competition and succession between diatom and dinoflagellate in the East China Sea. Sci. Tot. Environ. 574, 499–508.

Zhuo, X., 2018. Research on the basic characteristics of red tides along the coast of Fuzhou in the past ten years. Mar. Forecast 35 (4), 34–40 (in Chinese).